INTERLAMINAR/INTERFIBER FAILURE OF UNIDIRECTIONAL GFRP USED FOR WIND TURBINE BLADES

M. Leong[1], C.F. Hvejsel[1], E. Lund[2], O.T. Thomsen[2]*

[1]*Siemens Wind Power A/S, Assensvej 11, Aalborg, DK-9220, Denmark*
[2]*Department of Mechanical and Manufacturing Engineering, Aalborg University, Fibigerstræde 16, DK-9220, Aalborg East, Denmark*
**ott@m-tech.aau.dk*

Keywords: GFRP, material characterization, off-axis testing, failure criteria.

Abstract
A unidirectional glass fiber/epoxy composite material system used for wind turbine blades was characterized under multi-axial loading by cutting specimens in varying off-axis angles relative to the fiber direction. In addition, Iosipescu shear tests were performed on both symmetric and asymmetric specimens, where the latter were used to suppress premature axial splitting of the test specimens. The tests were performed in both the 1-2 and 1-3 material coordinate planes. Strain gauges and Digital Image Correlation were used to record the stress-strain responses. A new approach was used to define a "failure initiation strength" by analyzing the recorded stress-strain curves. The experimentally determined failure stresses were compared to the predictions of the maximum stress, Tsai-Wu and Northwestern University (NU) failure criteria. It was found that by using the approach of analyzing the stress-strain curve to define a point of material failure initiation, it was possible to obtain a good theoretical fit to the experimental data using both the Tsai-Wu and the NU failure criteria.

1 Introduction
The design and analysis of thick laminated composite structures require a thorough understanding of the behavior of the basic materials when they are subjected to various states of stress. Although fiber reinforced materials should be designed to carry the primary loads in the longitudinal fiber direction, multi-axial stress states are often induced in and near structural joints, load introduction areas, zones near boundary constraints, near geometric- and material discontinuities, such as ply dropoffs, and finally near structural/material defects such as in-plane and out-of-plane fiber misalignments. These multi-axial states of stress often involve combined transverse and shear loading, which can have a profound effect on the failure behavior of the material. Extensive research has been conducted on the general failure behavior and prediction of polymer matrix composites [1], and an abundance of different failure criteria of varying complexity and predictive capabilities have been proposed. Non-interactive and interactive criteria such as maximum stress, maximum strain [2] and the Tsai-Wu failure criteria [3] are typically used in industry. However, the first two do not take into account the effect of normal and shear stress interaction and the latter is not directly based on any physical mechanisms, despite performing well in many cases [1]. More advanced failure theories, such as the LaRC [4-6] and Puck [7,8] criteria, introduce additional fitting

parameters that need to be determined experimentally to better fit the test data. Furthermore, these criteria can be computationally expensive to use for large (real) scale composite structures. The Northwestern University (NU) failure theory proposed by Daniel et al. [9,10] attempts to model the interlaminar/interfiber failure of composites, is relatively inexpensive computationally, and does not require additional parameters other than the conventional strengths and stiffnesses of the unidirectional material. The NU theory has been shown to perform very well for carbon fiber composites (CFRP), but has not yet been tested extensively on glass fiber reinforced composites (GFRP).
The objective of the present investigation is to determine if existing failure theories can predict the failure behavior of typical wind turbine blade laminate configurations under realistic loading conditions. Experimental results are given of extensive static tensile, compressive and in-plane shear tests on a glass fiber/epoxy composite at various orientations with the principal material directions. These results provide the parameters needed for input in classical failure theories and characterizes the material behavior under combined normal and shear loading. The experimental data are compared with the predictions of several classical failure theories and the newly proposed NU criterion for interfiber/interlaminar failure. The paper concludes with an assessment of the predictive capabilities of the considered failure theories.

2 Material system and test specimens

The material investigated was a uni-directional E-glass/epoxy composite fabric. The dry fiber mat consists of 650 g/m^2 fibers in the 0 deg. direction and a 10 g/m^2 stitch in the in-plane 90 deg. direction. The stitch fibers primarily hold the 0 deg fiber bundles and have a negligible contribution to the stiffness and strength of the composite. Laminates of 2, 5 and 22 mm thickness were cast by stacking UD plies and infusing them with epoxy in a VARTM process. After infusion the laminates were allowed to cure at room temperature and were subsequently post cured in an oven. The fiber volume fraction of the finished laminates was measured to be approximately 58%. The material coordinate system used is shown in Figure 1. The "1-2 material plane" is the plane defined by the longitudinal (1) and transverse in-plane (2) axes and is also referred to as the interlaminar plane. The "1-3 material plane" is likewise defined by the longitudinal (1) and transverse through-thickness (3) axes and is also referred to as the interfiber plane.

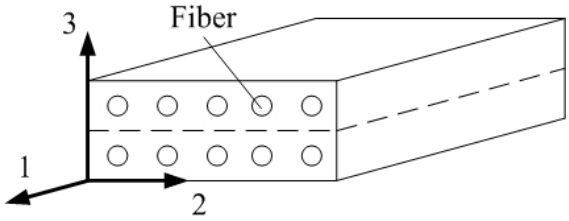

Figure 1. Material coordinate system used.

Tensile test specimens were cut from the 2 and 5 mm thick laminates in both rectangular and dog-bone shapes, and end tabs were bonded to the former according to the ASTM standard [11]. Specimens for compression testing were machined to a waisted-block geometry from the 22 mm plate with reduced cross section, guided by the ASTM standard [12]. In addition, for compression tests in the 1-3 plane, rectangular specimens were machined from the 22 mm plate as described by Daniel et al. [13]. Finally, V-notched Iosipescu specimen geometries, according to the ASTM standard [14], were chosen for shear testing in both the 1-2 and 1-3 planes, respectively.

3 Experimental methods

There are two primary objectives for the material characterization. The first was to determine the material stiffness and strength properties needed as input for the failure theories. These properties were determined by means of longitudinal and transverse tensile and compressive tests as well as shear tests. The second objective was to determine the material behavior under combined normal and shear loading. This was achieved by testing off-axis specimens. For all test configurations Digital Image Correlation was used to measure the surface strains on the test specimens. The measured strain maps were used to calculate an average strain over the gauge sections on the specimens.

4 Experimental results

4.1 Shear tests

The Iosipescu specimens produced average shear strengths, F_6 and F_5, of 80 MPa and 66 MPa, respectively. However, several types of matrix shear damage, in the form of both axial splits and delaminations in the through thickness direction were observed during the tests, see Fig.2, with the implication that the specimens were no longer loaded in pure shear. Axial splits are defined in the ASTM standard [14] and the accompanying load drop is not considered to be an ultimate failure load. The recorded shear stress vs. shear strain relations were strongly non-linear.

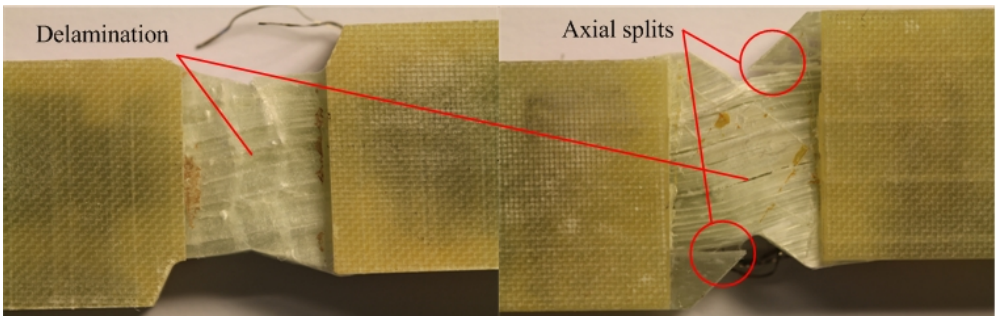

Figure 2. Iosipescu specimens after testing. Left: Asymmetric geometry, Right: Symmetric geometry. Note axial splits in the image on the right.

4.2 Tensile tests – along principal material directions and off-axis tests

The 90 deg. (transverse to the fiber direction) tension specimens failed at approximately 0.33% strain. Some specimens failed in the grip area, but this did not affect the measured strength, compared to the specimens that failed in the gauge section. The stress-strain curves for all tests were nearly linear up to failure. The mean tensile strength, F_{2t}, was measured to be 42 MPa. The average Young's modulus, E_2, was measured as 13.6 GPa.

All off-axis tension specimens failed along the fiber direction. Most specimens failed in the gauge zone. The 15 deg. off-axis specimens had a tendency to fail near the grips, and the fractures spanned both the gauge and transition zone. The stress-strain curves for the off-axis tension tests show mild non-linear behavior up to failure for the specimens with load orientations in the range of 15-75 degs. relative to the fiber direction as seen in Fig. 3. The tensile strength decreases with increasing off-axis angle, most significantly between the 15, 30 and 45 deg. specimens.

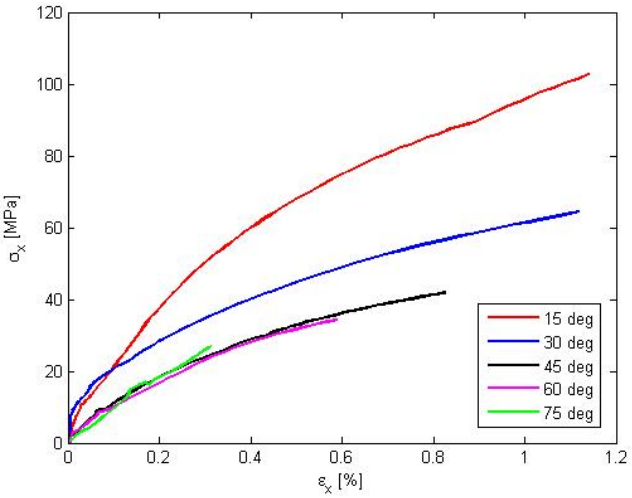

Figure 3. Typical stress-strain response for the off-axis tensile tests.

4.3 Compressive tests - along principal material directions and off-axis tests

The 90 deg. (transverse to the fiber direction) partially waisted compression specimens that were cut along the 2-direction failed at an average compressive stress of 130 MPa. The rectangular specimens cut in the 3-direction reached average compression strengths, F_{3c}, of 120 MPa and 123 MPa, for the 6x6x20 mm and 20x20x40 mm specimens, respectively . Both specimen types showed matrix failure patterns. The fracture plane orientation was measured between 38 deg. and 40 deg. For both specimen types, the average Young's modulus, E_3, was measured as 12.7 GPa. The stress-strain curves for all tests become noticeably non-linear above 1% strain, as shown in Fig. 4 for test specimens in the 3-direction.

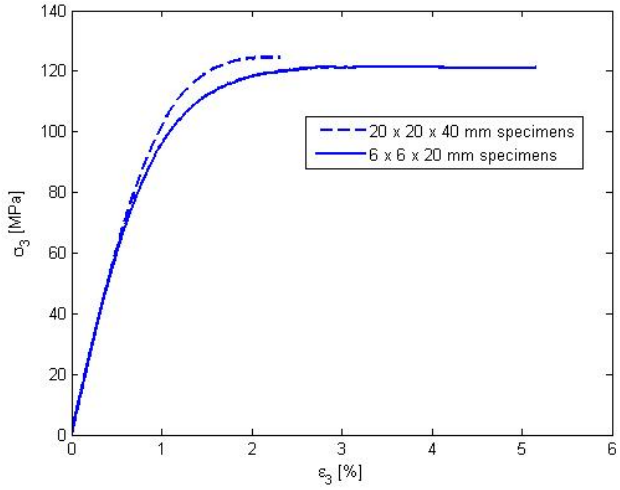

Figure 4. Typical stress-strain response in transverse compression in the 3-direction.

All off-axis test specimens, both in the 1-2 and 1-3 material coordinate planes, with the exception of the 15 deg. specimens, showed pronounced non-linear stress strain behavior over 0.5% strain, as illustrated in Fig. 5. As with the off-axis tensile tests, the compression strength decreases as the off-axis angle is increased, for the 1-2 plane specimens. This is especially pronounced between the 15 and 30 deg. off-axis angles. The strengths in the 1-3 plane on the other hand show a slight tendency to increase with increasing off-axis angles between 30 and 90 degs. Most specimens failed in the gauge or transition zone. The 15 deg. specimens failed mostly by kink-band formation. Some specimens showed fractures which spanned both the

gauge, transition and load introduction zones, and it was not possible to identify the exact location of failure initiation with the measurement methods used.

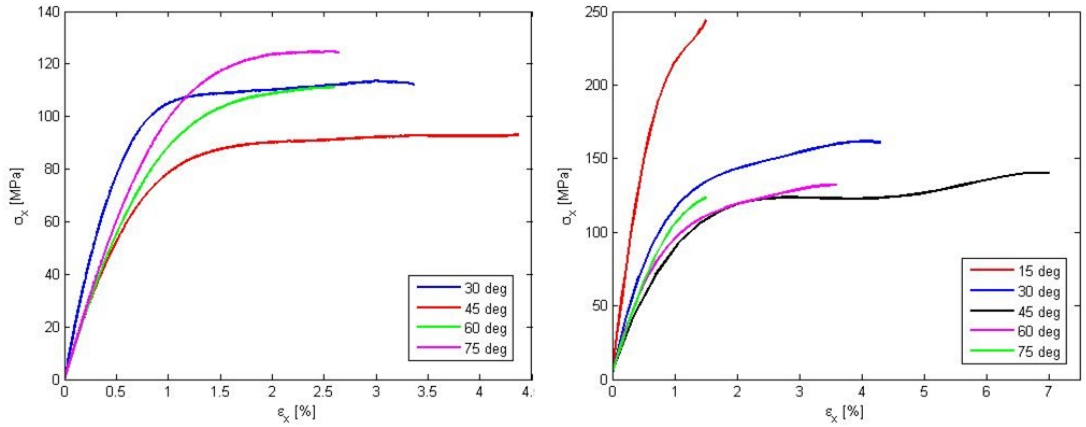

Figure 5. Typical stress-strain curves of off-axis compression specimens. Left: 1-3 material plane. Right: 1-2 material plane.

4.4 Determination of failure initiation strength

In an attempt to provide a more conservative shear strength estimate, that is, a "shear strength" that can used for design purposes to avoid matrix shear damage and plasticity, it is proposed to use a "failure onset strength", or "failure initiation strength", referring to the work of Lomov and co-workers [15-17], who found that the non-linear stress vs. strain behavior of NCF fabrics can be attributed to the initiation of micro damage. The stress-strain curves observed generally display various degrees of progressing non-linearity, where the non-linear material behavior is caused by progressive damage accumulation (matrix cracking, interface failure and fiber breakage) which leads to a gradual change (decrease) of the stiffness. The "failure initiation strength" is defined by the point on the stress-strain curve at which the relative change of the material stiffness is either largest or starts to increase significantly, which must be evaluated for each test type and depends mostly on how abruptly the material starts to exhibit non-linear response. In practice this is computed by dividing the stress-strain curve into a number of smaller segments. The slope of one segment is calculated by approximating the curve by a sequentially linear fit, and compared to the slope of the preceding segment as illustrated in Fig.6.

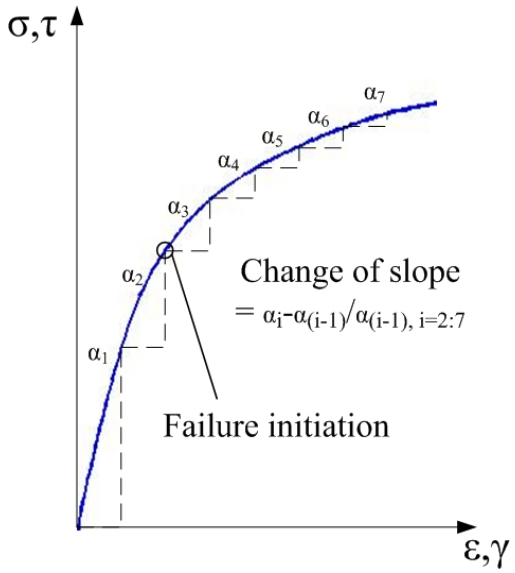

Figure 6. Graphical illustration of the proposed method to define "failure initiation strength" (or point) by the slope of the stress strain curve.

The slope of each segment is compared to the slope of the preceding segment by computing the percentage change. The point of failure initiation is defined as when this percentage change begins to increase significantly over the preceding values, which again depends on the size of the segments. For the material and measurement techniques presently used, a segment size between 0.05%-0.1% strain was found to represent the data adequately, and a stiffness change (decrease) of 50% was used to define the "failure initiation point/strength". This "failure initiation strength" can be regarded similarly as the yield strength of ductile materials, typically defined by the 0.2% offset point, which is based on empirical considerations. It is proposed to use this method for any kind of loading that produces a combined shear/normal stress state and whenever a more conservative strength estimation is required, assuming that the non-linear material behavior is caused by progressive damage accumulation as described above. The method was used on the Iosipescu shear tests, as well as the off-axis compression tests in the forthcoming section. See [18] for details.

5 Failure analysis

Several failure criteria were evaluated based on the obtained experimental results: the maximum stress criterion [2], the fully interactive Tsai-Wu criterion [3] and the failure mode based NU criterion [9-10].

The Northwestern University (NU) interfiber/interlaminar failure theory, proposed by Daniel et al. [9], is based on the assumption that the failure of composite materials is governed by the limiting microscopic strain in the interfiber/interlaminar region of the lamina. The NU theory consists of separate sub criteria for tension and compression failure, and furthermore separates the latter into compression and shear dominated failures, respectively. These three sub criteria are thus mostly applicable to anisotropic materials where the interlaminar failure can be distinguished into three separate and non/weakly interacting failure modes. The three sub criteria are given by the following equations in the 1-2 material plane [10]:

NUa/Compression dominated failure:

$$\left(\frac{\sigma_2}{F_{2c}}\right)^2+\left(\frac{\tau_6}{F_{2c}}\right)^2\cdot\left(\frac{E_2}{G_{12}}\right)^2=1 \tag{1}$$

NUb/Shear dominated failure:

$$\left(\frac{\tau_6}{F6}\right)^2+2\cdot\frac{\sigma_2}{F_6}\cdot\frac{G_{12}}{E_2}=1 \tag{2}$$

NUc/Tension dominated failure:

$$\frac{\sigma_2}{F_{2t}}+\left(\frac{\tau_6}{F_{2t}}\right)^2\cdot\left(\frac{E_2}{2\cdot G_{12}}\right)^2=1 \tag{3}$$

The three sub criteria given by Equations (1)-(3) are equally applicable to the 1-3 plane by interchanging subscripts 2 and 6 with 3 and 5, respectively. Equations (1)-(3) are used to create failure envelopes in the 1-2 and 1-3 planes, however, only for combined compression and shear in the 1-3 plane, due to the lack of experimental data.

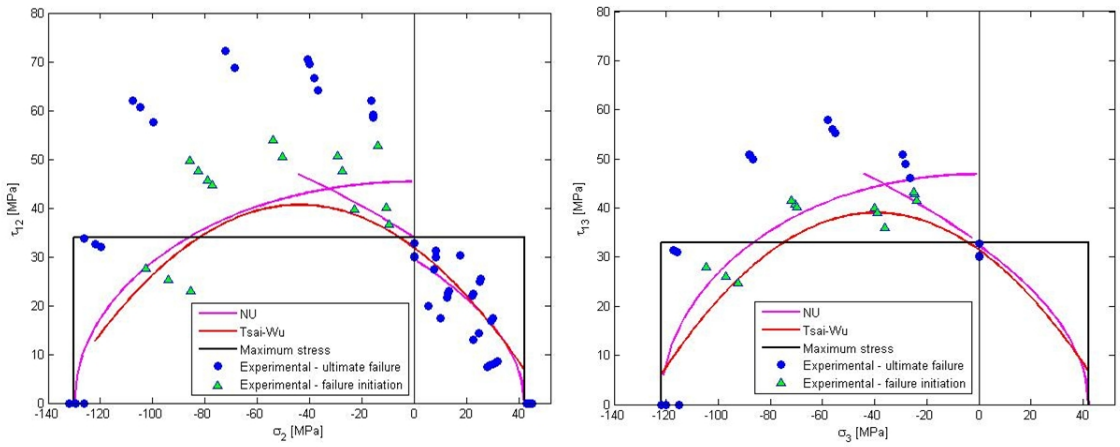

Figure 7. Comparison between experimental results and theoretical predictions in the 1-2 (left) and 1-3 (right) material planes, respectively, using the "failure initiation strength" definition.

As seen from Fig. 7, there does not appear to be a significant difference between the predictions of the NU and Tsai-Wu criteria in either the 1-2 or the 1-3 planes for the tested GFRP material. All failure theories also appear to be quite conservative compared to the experimentally determined ultimate failures. It should be noted that the NU failure curve between tension and shear dominated failures in the 1-2 plane (Fig. 7 left) is not continuous, which indicates a slight mismatch in the experimentally determined constitutive data, as the NU theory assumes a certain relation between the stiffness and strength of a material. However, the theoretical predictions provide a much better fit to the failure initiation data and as the method proposed in section 4.4 is aimed at identifying the initiation of micro damage, again referring to the work of Lomov and co-workers [15-17], it thus appears that by analyzing the stress/strain response of a material, it is possible to use existing failure criteria to determine the applied load at which the failure of the investigated materials initiates.

6 Summary and conclusions

A unidirectional glass/epoxy composite material was characterized in both the 1-2 and 1-3 material planes, subjected to uni-axial and combined compression and shear loading for both material planes, as well as combined tension and shear loading for the 1-2 plane. The failure modes were analyzed and it was observed that all specimens failed by interlaminar/interfiber failure, except the 15 deg. off-axis compression specimens in the 1-2 material plane, which failed by microbuckling and kink-band formation. The recorded stress-strain curves were used to define a point of failure initiation ("failure initiation strength"). This was done by identifying the point on the stress-strain curves at which the slope changes significantly or has a maximum value. The experimental results were used to evaluate three failure theories, of which the NU and Tsai-Wu criteria gave comparable results. The proposed method of analyzing the stress-strain response made it possible to use the existing failure theories to predict the point of damage initiation (or "failure initiation strength") with reasonable accuracy. For full details of the work presented herein see [18].

Acknowledgement

The work presented was conducted as part of an Industrial Ph.D. project carried out in collaboration between Siemens Wind Power A/S, Denmark and the Department of Mechanical and Manufacturing Engineering, Aalborg University, Denmark. The project has received partial sponsorship from the Danish Agency for Science, Technology and Innovation. The support received is gratefully acknowledged.

References

[1] Hinton, M.J., Kaddour, A.S., Soden, P.D., A comparison of the predictive capabilities of current failure theories for composite laminates, judged against experimental evidence, *Composites Science and Technology*, Vol. 62, pp.1725-1797 (2002)
[2] Kelly, A., *Strong Solids*, Clarendon Press, Oxford (1996).
[3] Tsai, S.W. and Wu, M., A General Theory of Strength for Anisotropic Materials, *Journal of Composite Materials*, Vol. 5, pp.58-80 (1971).
[4] Dávila, C.G., Camanho, P.P., Rose, C.A., Failure Criteria for FRP Laminates, *Journal of Composite Materials*, Vol. 39, No. 4 (2005).
[5] Pinho, S.T., Dávila, C.G., Camanho, P.P., Iannucci, L., Robinson, P. Failure models and criteria for FRP under in-plane or three-dimensional stress states including shear non-kinking: Part I: Development, *Composites Part A,* Vol. 37, pp. 63-73 (2006).
[6] Pinho, S.T., Iannucci, L., Robinson, P. Physically-based failure models and criteria for laminated fibre-reinforved composites with emphasis on fibre kinking: Part II: FE implementation, *Composites Part A,* Vol. 37, pp. 766-777 (2006).
[7] Puck, A., Schürmann, H., Failure analysis of FRP laminates by means of physically based phenomenological models, *Composites Science and Technology*, Vol. 58, pp. 1045-1067 (2002).
[8] Puck, A., Schürmann, H., Failure analysis of FRP laminates by means of physically based phenomenological models, *Composites Science and Technology*, Vol. 62, pp. 1633-1662 (2002).
[9] Daniel, I.M., Luo, J., Schubel, P.M, Werner, B.T., Interfiber/interlaminar failure of composites under multi-axial states of stress, *Composites Science and Technology,* Vol. 69, pp. 764-771 (2008).
[10] Daniel, I.M., Failure of Composite Materials, *Strain*, Vol. 43, pp 4-12 (2007).
[11] ASTM D 3039 – 08. *Standard test method for tensile properties of polymer matrix composite materials*.
[12] ASTM D 695 – 08. *Standard test method for compressive properties of rigid plastics*.
[13] Daniel, I.M., Luo, J.-J., Schubel, P.M., Three-dimensional characterization of textile composites, *Composites Part B,* Vol. 39, pp. 13-19 (2008)
[14] ASTM D 5379 – 05. *Standard test method for shear properties of composite materials by the V-notched beam method*.
[15] Carvelli, V., Gramellini, G., Lomov, S.V., Bogdanovich, A.E., Mungalov, D.D., Verpoest, I., Fatigue behavior of non-crimp 3D orthogonal weave and multi-layer plain weave E-glass reinforced composites, *Composites Science and Technology,* Vol. 70, pp. 2068-2076 (2010)
[16] Lomov, S.V., Bogdanovich, A.E., Ivanov, D.S., Mungalov, D., Karahan, M., Verpoest, I., A comparative study of tensile properties of non-crimp 3D orthogonal weave and multi-layer plain weave E-glass composites. Part 1: Materials, methods and principal results", *Composites: Part A,* Vol. 40, pp. 1134-1143 (2009)
[17] Ivanov, D.S., Lomov, S.V., Bogdanovich, A.E., Karahan, M., Verpoest, I., A comparative study of tensile properties of non-crimp 3D orthogonal weave and multi-layer plain weave E-glass composites. Part 2: Comprehensive experimental results, *Composites: Part A,* Vol. 40, pp. 1144-1157 (2009).
[18] Leong, M., Overgaard, L.T.T., Daniel, I.M., Lund, E. and Thomsen, O.T., Interlaminar/Interfiber Failure of Unidirectional GFRP Used for Wind Turbine Blades. *Journal of Composite Materials*. Accepted for publication (2012).